

Study of magnetic interactions in a spin liquid, $\text{Sr}_3\text{NiPtO}_6$ using density functional approach

Sudhir K. Pandey and Kalobaran Maiti*

Department of Condensed Matter Physics and Materials Science,

Tata Institute of Fundamental Research, Homi Bhabha Road, Colaba, Mumbai - 400 005, India

(Dated: November 21, 2018)

We investigate the magnetic interactions in $\text{Sr}_3\text{NiPtO}_6$, characterized to be a spin liquid using *ab initio* calculations. The results reveal a novel metal to insulator transition due to finite exchange interaction strength; the magnetic solutions (independent of magnetic ordering) are large band gap insulators, while the non-magnetic solution is metallic. The Ni moment is found to be large and the coupling among intra-chain Ni moments is antiferromagnetic unlike other compounds in this family. These results, thus, reveal the importance of intra-chain antiferromagnetic interaction in addition to geometrical frustration to derive spin liquid phase.

PACS numbers: 75.30.Et, 75.50.Mm, 71.70.Gm, 75.20.Hr

Geometrical frustration in antiferromagnetically coupled systems often prevents long range order. Here, the magnetic moments are strongly correlated, still they remain paramagnetic even at zero temperature. Such systems are called *spin liquids*. Certain crystal structures e.g. Kagomé lattice, pyrochlores *etc.* consisting of triangular units are frustrated and are favorable to generate this phase. However, spin liquid phase is barely observed experimentally as the long range order can be achieved in such frustrated systems via small perturbations due to disorder, pressure, application of external fields *etc.*

Recently, a new class of compounds, $\text{AE}_3\text{MM}'\text{O}_6$ (AE = alkaline earths, M and M' are transition metals) is found having geometrical frustration. The crystal structure is rhombohedral K_4CdCl_6 type (space group $R\bar{3}c$) as shown in Fig. 1. It contains one-dimensional (1D) chains along c -axis consisting of alternating MO_6 trigonal prisms and $M'\text{O}_6$ octahedra connected by face sharing. In the ab -plane, the chains form a triangular lattice. Thus, these systems exhibit fascinating electronic and magnetic properties characteristic of 1D chains as well as those due to geometrical frustration in the ab -plane. Many compounds in this class are synthesized and studied extensively due to the finding of varieties of interesting properties involving geometrical frustration^{1,2,3,4,5,6,7,8,9,10,11,12,13,14,15,16,17,18} unlike other quasi-one dimensional systems having no frustration.^{19,20,21,22}

Interestingly, only $\text{Sr}_3\text{NiPtO}_6$ exhibit spin liquid behavior.¹ Analogous compounds $\text{Sr}_3\text{NiRhO}_6$ ¹ and $\text{Sr}_3\text{CuPtO}_6$ ² exhibit long range order as the other compounds in this family does.^{3,4,5,6} In these later systems, geometrical frustration is manifested as partially disordered antiferromagnetic phase, where two thirds of the chains are antiferromagnetically coupled and the third one is incoherent. Several contrasting suggestions exists in the literature to explain the absence of magnetic order in $\text{Sr}_3\text{NiPtO}_6$. For example, comparison of $\text{Sr}_3\text{NiPtO}_6$ and $\text{Sr}_3\text{CuPtO}_6$ indicated that Ni^{2+} could be in a singlet state.² However, Ni^{2+} in a similar compound, $\text{Sr}_3\text{NiRhO}_6$ possess large magnetic moment ($S =$

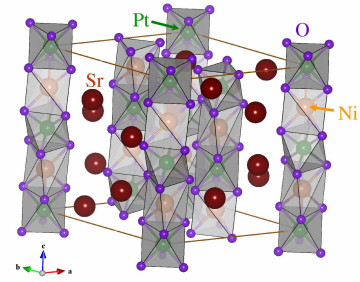


FIG. 1: (Color online) The crystal structure of $\text{Sr}_3\text{NiPtO}_6$. Quasi-one dimensional chains are shown by shaded regions.

1 state).^{1,6} Thus, the absence of spin liquid phase in these frustrated systems as well as its anomaly in $\text{Sr}_3\text{NiPtO}_6$ is puzzling. Here, we show that Ni moment is large and couple antiferromagnetically along the chain unlike other compounds.^{1,6,23} This is probably important to derive spin liquid phase in this compound. In addition, we observe a novel magnetization induced metal to insulator transition.

The nonmagnetic and magnetic GGA (generalized gradient approximation) electronic structure calculations were carried out using *state-of-the-art* full potential linearized augmented plane wave (FPLAPW) method.²⁴ The spin orbit coupling for Ni and Pt were considered in the calculations. The lattice parameters and atomic positions used in the calculations are taken from the literature.² The Muffin-Tin sphere radii were chosen to be 2.33, 2.19, 2.01, and 1.78 a.u. for Sr, Ni, Pt, and O, respectively. For the exchange correlation functional, we have adopted recently developed GGA form by Wu *et al.*²⁵ The convergence was achieved by considering 512 k points within the first Brillouin zone and the error bar for the energy convergence was set to be smaller than 10^{-4} Rydberg/cell.

Calculated energy bands are shown in Fig. 2; the left and right panels show the band dispersions corresponding to non-magnetic and ferromagnetic solutions, respec-

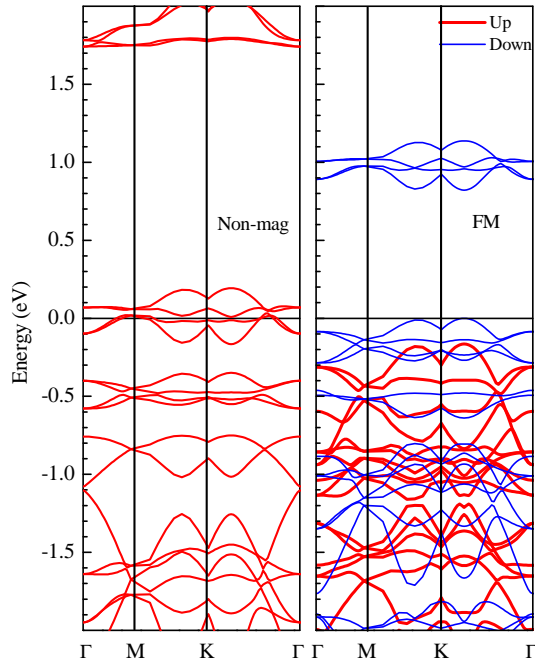


FIG. 2: (Color online) Band dispersions along different symmetry directions of the first Brillouin zone for nonmagnetic and ferromagnetic solutions. Fermi level is denoted by zero in the energy scale.

tively. The non-magnetic solution clearly correspond to a metallic ground state with large contribution at the Fermi level, ϵ_F represented by 'zero' in the energy scale. There are four bands lying within ± 0.1 eV of ϵ_F . At the Γ and M points, the bands just above and below the ϵ_F are two fold degenerate. The separation of these bands are largest at Γ point (~ 0.16 eV) and lowest at M point (~ 0.04 eV). The degeneracy of these bands is lifted along MK direction.

In the ferromagnetic solution, the up-spin energy bands move away from the Fermi level, towards lower energies. The Fermi level appears at the top of the down spin bands. The energy gap in the down spin channel is about 0.8 eV, which is much smaller than the gap of ~ 2.5 eV in the up spin channel. Thus, in this phase, the electronic conduction will be spin-polarized even in the insulating phase in a large temperature range. The insulating gap of about 0.8 eV appears along the MK and ΓK directions. The band gaps at Γ , K and M points are found to be about 0.96, 1 and 1.1 eV, respectively.

The most notable observation here is the manifestation of insulating phase due to magnetization in a non-magnetic metal. It is observed that antiferromagnetic phase may lead to metal-insulator transition due to change in lattice translational symmetry (supercell symmetry), thereby splitting the Brillouin zone. The other effect observed (e.g. in giant magnetoresistive materials) is a transition from paramagnetic insulating phase to fer-

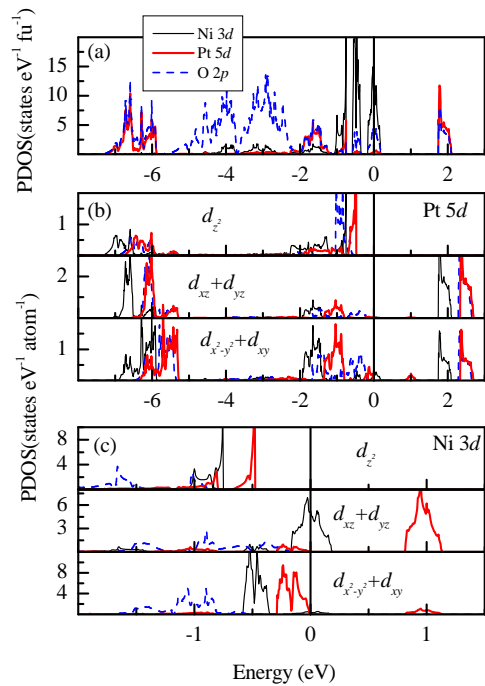


FIG. 3: (Color online) (a) The partial density of states (PDOS) corresponding to Ni 3d (thin solid lines), O 2p (dashed lines) and Pt 5d (thick solid lines) states for non-magnetic solution. In (b) and (c), we show d_{z^2} (upper panel), $d_{xz} + d_{yz}$ (middle panel) and $d_{x^2-y^2} + d_{xy}$ (lower panel) PDOS for Pt 5d and Ni 3d states, respectively. Up and down spin PDOS are shown by dashed and thick solid lines, respectively. In each case, half of the non-magnetic PDOS is shown by thin solid line for comparison.

romagnetic metallic phase; here the ferromagnetism leads to a metallic conduction. The present case is completely opposite revealing a large band gap insulating ferromagnetic phase in a non-magnetic metal.

In order to understand the effect, we plot the character of various energy bands in Fig. 3. The degeneracy of Ni 3d in NiO_6 trigonal prisms and Pt 5d orbitals in PtO_6 octahedra is lifted due to the corresponding crystal field effect. We have defined the axis system such that the z -axis lies along c -axis, and x - & y -axes are in the ab -plane (see Fig. 1). The crystal field splitting of the Ni 3d and Pt 5d levels are evident in Fig. 3(a), where we show the Ni 3d, Pt 5d and O 2p partial density of states (PDOS) obtained from non-magnetic solution. Pt 5d dominated bonding and antibonding energy bands appear in the energy ranges -7 to -5 eV and -2.5 to -1 eV, respectively. O 2p contributions appear primarily between -2 to -5 eV. Energy bands having dominant Ni 3d character shown by thin solid line appear in the vicinity of the Fermi level. Trigonal prismatic crystal field around the Ni site leads to three distinct energy bands having d_{z^2} , $(d_{x^2-y^2}, d_{xy})$ and (d_{xz}, d_{yz}) character as seen in Figs. 3(c). Clearly, the ground state is metallic and the electronic density of

states at the Fermi level are primarily contributed by Ni $3d_{xz} + d_{yz}$ states.

In Fig. 3(b), we show the spin polarized Pt $5d$ PDOS. Both the spin channels of Pt $5d$ states are partially occupied and the insulating gap in the up spin channel is essentially decided by the $5d$ states, which is found to be about 2.5 eV. From the total electron count, we find that the Pt has 6 electrons in the $5d$ bands; the valence state is $4+$. These 6 electrons occupy t_{2g} spin-orbitals making it completely filled. Since all these energy bands appear at much lower energies, an exchange splitting of about 0.6 eV observed for Pt $5d$ states does not push the down spin bands enough towards the Fermi level to make them partially filled. Thus, the Pt $5d$ possess weak magnetic moment presumably induced by Ni $3d$ moments.

Spin polarized calculations exhibit large exchange splitting (about 1 eV) in all the spin-orbitals corresponding to Ni $3d$ electronic states. Such a large exchange correlation does not affect the insulating state of the d_{z^2} and $(d_{x^2-y^2}, d_{xy})$ energy bands. The spin degeneracy lifting of (d_{xz}, d_{yz}) bands leads to a gap of about 0.8 eV at ϵ_F . Since, Ni^{3+} has 8 electrons in the d band, the down spin band becomes completely empty due to spin polarization. Thus, the Hund's coupling drives the system towards insulating ground state.

It is to note here that capturing insulating ground state in most of the oxides containing $3d$ transition metals requires consideration of on-site Coulomb interaction strength, U among $3d$ electrons. Correlation effect is also important in higher d systems.^{26,27} This is also the case in $\text{Sr}_3\text{NiRhO}_6$.⁶ However, in the present case, on-site Coulomb correlation among d electrons is not necessary to determine the electronic properties of $\text{Sr}_3\text{NiPtO}_6$. We have verified this by including U in our calculations (LSDA+ U); U corresponding to Ni $3d$ electrons was varied upto 7 eV and that corresponding to Pt $4d$ electrons upto 4 eV. We did not observe any change in the electronic structure that will influence the electronic and magnetic properties except an enhancement in the energy gap with the increase in U maintaining the insulating ground state. The Ni moments are also found to be very close to the LSDA results. This is consistent with the expectations for an insulating system.

The total converged energy for the ferromagnetic solution is found to be ~ 781 meV/fu lower than that for the non-magnetic solution. This clearly provides evidence against the non-magnetic phase for this system as predicted in previous studies.² The magnetic moment centered at Ni sites is significantly large ($\sim 1.5 \mu_B$). The magnetic moment at Pt site turns out to be negligibly small ($\sim 0.02 \mu_B$) indicating that Pt is in low spin state in the octahedral symmetry. The total magnetic moments per formula unit is found to be about $2 \mu_B$.

In order to investigate the effect of spin-orbit coupling (SOC) on the magnetic states of the Ni and Pt, we performed FM GGA calculations including SOC for both the atoms. This calculation converges again to the insulating ground state. The spin part of the magnetic

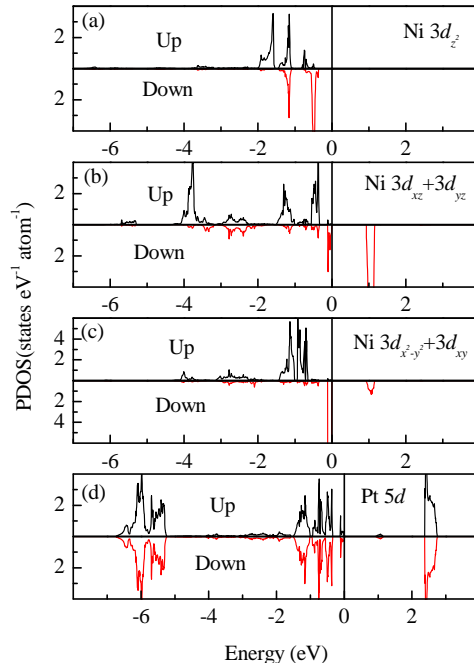


FIG. 4: (Color online) Up and down spin PDOS corresponding to (a) $\text{Ni}3d_{z^2}$ (b) $\text{Ni}3d_{xz} + d_{yz}$, (c) $\text{Ni}3d_{x^2-y^2} + d_{xy}$, and Pt $5d$ states for antiferromagnetic solution.

moments do not get affected by the SOC. However, SOC induces about $0.16 \mu_B$ orbital magnetic moments at Ni site. The direction of orbital and spin parts of magnetic moments are same, which is as per the Hund's rule. The orbital part of magnetic moment for Pt atom is found to be very small ($0.02 \mu_B$). This result is surprising as the effect of SOC is expected to be significantly larger for heavier Pt atom in comparison to lighter Ni atom. The observance of negligibly small orbital magnetic moment for Pt may be attributed to the fully filled t_{2g} orbitals. The relatively small value of orbital part of magnetic moment in comparison to spin part clearly indicates that the magnetic properties of $\text{Sr}_3\text{NiPtO}_6$ compound is primarily determined by the spin dynamics associated to Ni $3d$ electrons.

It is already well known that magnetic interactions can be captured well via *ab initio* calculations.²⁸ In order to learn the nature of magnetic interaction among Ni atoms, we calculated the electronic structure for antiferromagnetic coupling among neighboring intra-chain Ni atoms. The energy of this solution is found to be about 5 meV/fu less than that for the FM solution indicating that antiferromagnetic interaction provides more stability to the system, which is consistent with magnetization data.¹ The calculation gives almost the same magnetic moments ($\sim 1.5 \mu_B$) as observed before; the net magnetic moment is close to zero. This Ni moment is very close to that found in $\text{Sr}_3\text{NiRhO}_6$.⁶

Now we discuss the effect of antiferromagnetic interac-

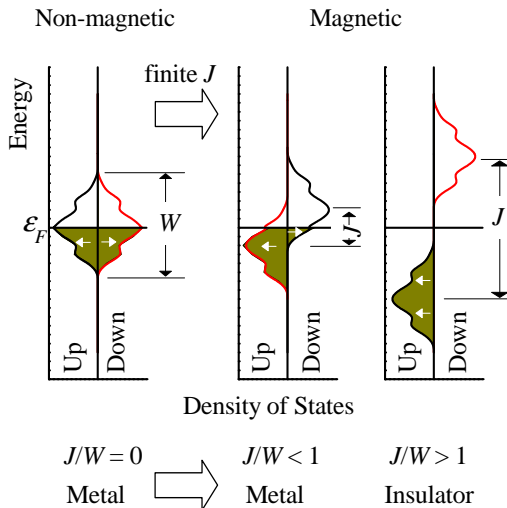


FIG. 5: A demonstration of how an insulating phase appears due to finite exchange coupling strength, J . For $J/W > 1$ (W = bandwidth) the system becomes insulating and $J/W < 1$ it remains metallic.

tion on the electronic structure of the compound. Since the energy distribution of the density of states for both the nonequivalent Ni sites (due to antiparallel ordering) are almost identical, we plot the partial density of states corresponding to only one Ni site in Fig. 4. The $3d$ orbitals having different symmetries are plotted in separate panels of the figure for clarity. The density of states clearly manifest again the insulating phase. The band gap of about 1 eV is observed in the down spin channel as in the ferromagnetic case and the gap in up spin channel is much higher. The Pt $3d$ PDOS appear within -1.7

eV from the Fermi level. The small exchange splitting observed in ferromagnetic solution is now absent. This is expected as each Pt has one up-spin and one down-spin Ni neighbor. Therefore, the induced moment due to finite orbital overlaps will be vanished. Similar behavior is also seen for O $2p$ PDOS.

In summary, we show an example of emergence of an insulating phase from a metallic phase due to finite exchange interaction strength. The metal to insulator transition, here, is driven by exchange splitting and independent of magnetic coupling among moments located at different sites. This is demonstrated schematically in Fig. 5. E.g. in a simple model consisting of half filled bands, if the exchange splitting J is larger than the bandwidth W ($J/W > 1$) the system becomes insulating purely due to the exchange interactions. $J/W < 1$ corresponds to metallic ground state. Such a metal-insulator transition can be achieved experimentally by tuning the bandwidth as often done in correlated electron systems via change in bond-angles and/or exchange interaction strength via chemical substitutions.

The Ni moments are found to be large in $\text{Sr}_3\text{NiPtO}_6$. Consideration of electron correlation appears to be not necessary to determine the electronic properties and magnetic moments. The *ab initio* results reveal that Ni moments are coupled antiferromagnetically along the chain. As the inter-chain interactions are complicated (M -O-O- M super superexchange interaction), intra-chain interactions become important and probably play the key role for the spin liquid phase.

The authors acknowledge Prof. E.V. Sampathkumaran, TIFR, India for drawing our attention towards this compound and useful discussions.

* Electronic mail: kbmaiti@tifr.res.in

- ¹ N. Mohapatra, K. K. Iyer, S. Rayaprol, and E. V. Sampathkumaran, Phys. Rev. B **75**, 214422 (2007).
- ² J. B. Claridge, R. C. Layland, W. H. Henley, and H-C z Loye, Chem. Mater. **11**, 1376 (1999).
- ³ H. Wu, M. W. Haverkort, Z. Hu, D. I. Khomskii, and L. H. Tjeng, Phys. Rev. Lett. **95**, 186401 (2005).
- ⁴ H. Wu, Z. Hu, D. I. Khomskii, and L. H. Tjeng, Phys. Rev. B **75**, 245118 (2007).
- ⁵ D. Flahaut, S. Hébert, A. Maignan, V. Hardy, C. Martin, M. Hervieu, M. Costes, B. Raquet, and J.M. Broto, Eur. Phys. J B **35**, 317 (2003).
- ⁶ S. K. Pandey and K. Maiti, Phys. Rev. B **78**, 045120 (2008).
- ⁷ E. V. Sampathkumaran and A. Niazi, Phys. Rev. B **65**, 180401(R) (2002).
- ⁸ S. Agrestini, C. Mazzoli, A. Bombardi, and M.R. Lees, Phys. Rev. B **77**, 140403(R) (2008).
- ⁹ S. Niitaka, K. Yoshimura, K. Kosuge, M. Nishi, and K. Kakurai, Phys. Rev. Lett. **87**, 177202 (2001).
- ¹⁰ S. Niitaka, H. Kageyama, M. Kato, K. Yoshimura, and K. Kosuge, J. Solid State Chem. **146**, 137 (1999).

- ¹¹ K. E. Stitzer, W. H. Henley, J. B. Claridge, H. -C. zur Loye, and R. C. Layland, J. Solid State Chem. **164**, 220 (2002).
- ¹² K. Sengupta, S. Rayaprol, K. K. Iyer, and E. V. Sampathkumaran, Phys. Rev. B **68**, 012411 (2003).
- ¹³ M. -H. Whangbo, D. Dai, H. -J. Koo, and S. Jobic, Solid State Commun. **125**, 413 (2003).
- ¹⁴ R. Vidya, P. Ravindran, H. Fjellvåg, and A. Kjekshus, Phys. Rev. Lett. **91**, 186404 (2003).
- ¹⁵ E. V. Sampathkumaran, N. Fujiwara, S. Rayaprol, P. K. Madhu, and Y. Uwatoko, Phys. Rev. B **70**, 014437 (2004).
- ¹⁶ R. Frésard, C. Laschinger, T. Kopp, and V. Eyert, Phys. Rev. B **69**, 140405(R) (2004).
- ¹⁷ K. Takubo, T. Mizokawa, S. Hirata, J.-Y. Son, A. Fujimori, D. Topwal, D. D. Sarma, S. Rayaprol, and E.-V. Sampathkumaran, Phys. Rev. B **71**, 073406 (2005).
- ¹⁸ J. Sugiyama, H. Nozaki, Y. Ikeda, P. L. Russo, K. Mukai, D. Andreica, A. Amato, T. Takami, and H. Ikuta, Phys. Rev. B **77**, 092409 (2008).
- ¹⁹ P. Gambardella, A. Dallmeyer, K. Maiti, M.C. Malagoli, W. Eberhardt, K. Kern, and C. Carbone, Nature **416**, 301 (2002).

- ²⁰ K. Maiti and D.D. Sarma, Phys. Rev. B **58**, 9746 (1998).
- ²¹ K. Maiti, D.D. Sarma, T. Mizokawa, and A. Fujimori, Europhys. Lett. **37**, 359 (1997).
- ²² K. Maiti, P. Mahadevan, and D.D. Sarma, Phys. Rev. B **59**, 12457 (1999).
- ²³ S. Aasland, H. Fjellvåg, and B. Hauback, Solid State Commun. **101**, 187 (1997).
- ²⁴ P. Blaha, K. Schwarz, G.K.H. Madsen, D. Kvasnicka, and J. Luitz, WIEN2k, An Augmented Plane Wave + Local Orbitals Program for Calculating Crystal Properties (Karlheinz Schwarz, Techn. Universität Wien, Austria), 2001. ISBN 3-9501031-1-2.
- ²⁵ Z. Wu and R. E. Cohen, Phys. Rev. B **73**, 235116 (2006).
- ²⁶ K. Maiti and R.S. Singh, Phys. Rev. B **71**, 161102(R) (2005); K. Maiti, R. S. Singh, and V. R. R. Medicherla, Phys. Rev. B **76**, 165128 (2007).
- ²⁷ R. S. Singh, V. R. R. Medicherla, K. Maiti, and E. V. Sampathkumaran, Phys. Rev. B **77**, 201102(R) (2008).
- ²⁸ D. D. Sarma, N. Shanthi, S. R. Barman, N. Hamada, H. Sawada, and K. Terakura, Phys. Rev. Lett. **75**, 1126 (1995); K. Maiti, Phys. Rev. B **73**, 235110 (2006), *ibid.*, Phys. Rev. B **73**, 115119 (2006), *ibid.*, Phys. Rev. B **77**, 212407 (2008).